

Nominal Range Error Analysis of BDS for ARAIM

Hengwei Zhang, Yiping Jiang

Interdisciplinary Division of Aeronautical and Aviation Engineering, The Hong Kong Polytechnic University

BIOGRAPHY

Hengwei Zhang is currently a PhD student in the Interdisciplinary Division of Aeronautical and Aviation Engineering at The Hong Kong Polytechnic University. He received his B.E. degree in the School of Mechatronic Engineering from China University of Mining and Technology in 2015 and M.E. degree in the School of Mechanical Engineering from Xi'an Jiaotong University in 2018. His research interests include integrity monitoring and precise positioning approaches.

Dr. Yiping Jiang is an assistant professor of the Interdisciplinary Division of Aeronautical and Aviation Engineering at The Hong Kong Polytechnic University. She obtained her Ph.D. degree from the University of New South Wales in 2014 with research interests including precise positioning and integrity monitoring technologies. She currently lectures on avionics systems, guidance and navigation for undergraduate students.

ABSTRACT

The Advanced Receiver Autonomous Integrity Monitoring (ARAIM) requires a minimum performance level of the satellite constellation that is used for aircraft navigation. The distribution of the satellite Signal-In-Space (SIS) range error needs to be sufficiently characterized considering the correlation in error terms. The nominal range error for 14 BDS-2 and 11 BDS-3 satellites and the correlation of orbit and clock errors are analyzed based on one-year data of broadcast and precise ephemerides. Results show significant differences in the nominal range error performance among three different types of satellites of GEO, IGSO and MEO and different manufacturers. The service history is broken down into monthly dataset to analyze the variation of single satellite performance and BDS-2 is compared with BDS-3 from multiple aspects. The URE is characterized and one-sigma value is 9.4m, 5.8m and 4.9m for GEO, IGSO and MEO, respectively. Based on the correlation analysis, orbit error components show significant disparity in the harmonic period between satellite types. Like orbit error components, the large difference also exists in clock error regarding convergence time. Independent sampling interval is estimated with the time interval ranging from 44 to 67, 14 to 15 and 11 to 12 hours for GEO, IGSO and MEO, respectively.

INTRODUCTION

With the modernization of GPS and other global navigation satellite systems (GNSS) becoming operational, e.g. GLONASS, Galileo and BDS, the Advanced Receiver Autonomous Integrity Monitoring (ARAIM) has been developed by taking advantage of the dual-frequency and multi-constellation measurements. ARAIM as an airborne application can support LPV-200 service globally. Satellite navigation signals may be failed in the process of production, transmission and reception. ARAIM relies on consistency check of redundant measurements for fault detection and exclusion. The protection level is then used to bound the undetected errors using parameters from the Integrity Support Message (ISM), which is generated from ground monitoring stations [1]. The parameters in ISM include the User Range Accuracy (URA), the User Range Error (URE),

the nominal bias, the probability of single satellite and of constellation-wide faults [2]. The first three parameters describe a modeled distribution of error terms as an overbound of the true distribution. The historical data is used to set bounds for mean and standard deviation values of errors.

There are abundant works on the evaluation of GNSS performance during their service histories. The statistical characteristics of GPS satellite orbit and clock errors were described during its service history from 2008 until the end of 2014 with detailed analysis about several major fault events [3]. The performance of GLONASS and GPS was compared and the URAs of GLONASS and GPS were bounded as 18m and 2.4m respectively [4]. Nine satellites of Galileo were also analyzed to characterize range errors based on more than one-year data [5]. Further studies involved the correlation and independence of sample data for new constellations where available data is limited. The effects of orbit and clock errors' autocorrelation on the URE bounding for GPS and Galileo satellites were analyzed [6] [7]. One month's data of BeiDou was analyzed to calculate the averaged URE for three different orbital altitude satellites with two BDS-2 MEO satellites [8]. The short characterized period data cannot reflect the actual statistical distribution of error terms and too few satellites shall not be representative of the whole constellation performance. More MEO satellites, especially BDS-3 satellites, and longer time data need to be analyzed. Meanwhile, correlation of time variant error components should also be concerned for BDS. The URE value is comprehensively evaluated for 14 BDS-2 and 11 BDS-3 satellites and the correlation of error terms is further analyzed based on a one-year time span in the paper.

This paper is organized as follows. Firstly, methods for evaluating URE and correlation of error components are described. Secondly, analysis results for error components and individual satellite are provided and discussed. Meanwhile, monthly dataset is analyzed to show the variation of single satellite performance and BDS-2 is compared with BDS-3 from multiple aspects. Finally, the correlation of orbit and clock errors is assessed, and the time between independent samples is estimated for GEO, IGSO and MEO.

CALCULATION METHOD OF BDS URE AND AUTOCOVARIANCE

When evaluating BDS performance, the uniqueness of the system and the consistency of orbit and clock information should be considered. The space segment of BDS uses a hybrid constellation composed of three kinds of satellites: GEO, IGSO and MEO satellites with different orbital altitudes. Besides, there are still several aspects needed to be discussed like time and reference systems, antenna offset and clock correction.

Broadcast and precise ephemerides are needed when calculating the satellite orbit and clock errors. The broadcast ephemeris is downloaded from the center of Multi-GNSS Experiment (MGEX) of the International GNSS Service (IGS) with RINEX 3 format. The precise ephemeris is generated by IGS Wuhan analysis center and made available through public database with few centimeters range accuracy that is assumed as the true value [9]. For time and reference systems, the precise ephemeris is referred to the GPS time system while broadcast ephemeris is referred to the BDS time system. A BDS-GPS time offset of 14 seconds needs to be removed. Even though the reference system of GPS is World Geodetic System 1984 (WGS84) and BDS uses China Geodetic Coordinate System 2000 (CGCS2000), error between these two reference systems is around a few centimeters which can be ignored [10].

Even if the reference coordinate systems of broadcast and precise ephemerides are consistent, the original reference point of coordinate system is not same. Precise ephemeris provides the center-of-mass (CoM) coordinates of the respective satellite. Broadcast ephemeris, in contrast, is referred to the satellite antenna phase center (APC) [11]. Before 2017, both laser ranging

residuals and ephemeris comparisons indicated that broadcast ephemeris of BDS is referred to the CoM and a zero offset is adopted [12]. After 2017, the broadcast ephemeris of BDS updates the reference point as APC and the IGS reference values for the antenna offset are used [13].

Except the antenna offset correction, clock offset of precise and broadcast ephemerides cannot be compared directly because of the different signal combination employed in their generation. The broadcast ephemeris of BDS is referred to the single-frequency B3 signal and the precise ephemeris is based on the ionosphere-free B1/B2 signals [14]. A corresponding correction of the BDS broadcast clocks is defined as

$$TGD_{brdc} = \frac{f_1^2}{f_1^2 - f_2^2} TGD_1 - \frac{f_2^2}{f_1^2 - f_2^2} TGD_2 \quad (1)$$

where TGD_{brdc} is the time group delay correction for the broadcast clock, TGD_1 is the time group delay of B1 frequency and TGD_2 is the time group delay of B2 frequency. f_1 and f_2 are the frequencies of B1I and B2I, respectively.

Also, there is a common bias of all satellites due to the different time scales, which varies from time to time. For this bias, the average broadcast-minus-precise clock values of all satellites in a constellation is computed at each epoch. Every satellite clock offset is corrected by this averaged value [10].

SISRE and error autocovariance computation

The global average URE is root-mean-square (RMS) statistical value of the projection error of satellite orbit and clock errors on the signal propagation direction [15]. The impact of orbit errors can be divided into three directions, i.e. radial, along-track and cross-track on the line-of-sight. The RMS formula of URE is defined as [16]

$$URE = \sqrt{(\alpha \cdot R - c \cdot T)^2 + \beta \cdot (A^2 + C^2)} \quad (2)$$

where R is the radial error, A is the along-track error, C is the cross-track error, T is the clock error, c is the speed of light, α and β are the weight factors depending on the altitude of satellite.

Considering the three types of satellites for BDS, i.e. GEO, IGSO and MEO, the combined orbit and clock URE calculation models are further specified [17]

$$URE_{GEO/IGSO} = \sqrt{(0.99 \cdot R - c \cdot T)^2 + \frac{1}{127} (A^2 + C^2)} \quad (3)$$

$$URE_{MEO} = \sqrt{(0.98 \cdot R - c \cdot T)^2 + \frac{1}{54} (A^2 + C^2)} \quad (4)$$

The autocovariance provides a temporal representation of the correlation between the error and a delayed copy of itself. Typically, the autocovariance function is normalized by the sample variance [7]. For a given random process $x(t)$, the autocovariance C_{xx} function is defined as

$$C_{xx}(\tau) = E[x(t)x(t + \tau)] - \mu_x^2 \quad (5)$$

where μ_x is the mean value of the random variable $x(t)$.

To provide estimation of valid independent samples, the following equations are used to calculate the time between independent samples [7]

$$\frac{N_r}{N} = \frac{\sigma_x^2}{\sum_{N-k}^N (1 - \frac{|k|}{N}) C_{xx}(k)} \quad (6)$$

$$T_r = \frac{T}{\frac{N_r}{N}} \quad (7)$$

where N_r is the number of effectively independent samples, N is the total number of collected samples and σ_x^2 is the variance value of the error data $x(t)$. T_r is the time between independent samples and T is the selected sample interval.

RESULT AND DISCUSSION

As of January 2019, the following 25 BDS-2 and BDS-3 satellites have been used including GEO, IGSO and MEO with available data: four GEO satellites (C016, C018, C006 and C011), seven IGSO satellites (C005, C007, C008, C009, C010, C017 and C019) and fourteen MEO satellites (C012, C013, C015, C201, C202, C206, C205, C209, C210, C212, C211, C203, C024 and C207) [18]. The study presented in the paper includes BDS service data from January 2019 until December 2019 during the constellation deployment. The satellite orbit and clock errors are time variant components. C012 satellite is selected to show varying of orbit and clock errors with time on January 1, 2019 in Figure 1.

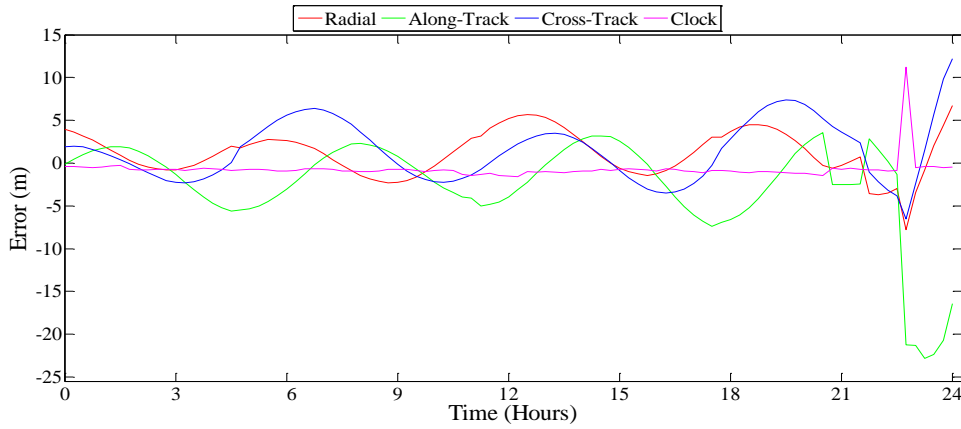


Figure 1: Orbit and clock errors for C012 on January 1, 2019

For orbit and clock errors, due to the fact that range errors appear quasi-gaussian distribution [3] and given the mathematical simplicity afforded when convolving errors using a gaussian model [4], the gaussian model is used to fit observation samples.

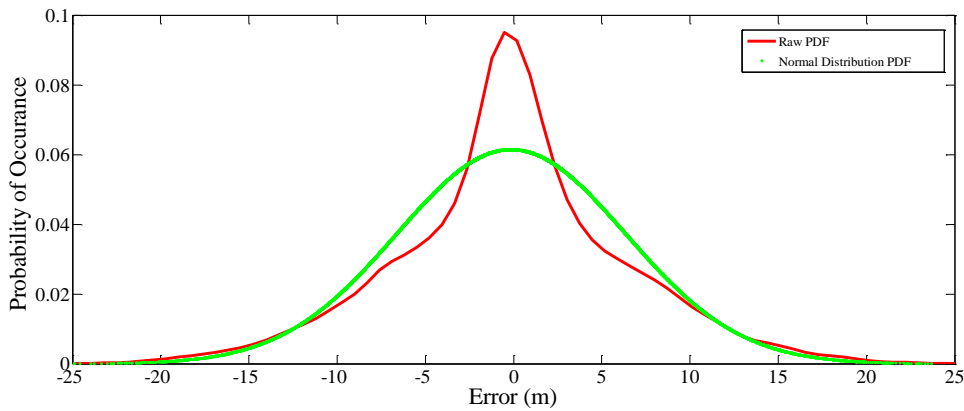


Figure 2: Radial error distribution

Figure 2 shows the observed probability density function (PDF) for the radial projected error of C012 satellite. The red line shows the PDF of raw data and green line is the PDF of observation samples fitted by the normal distribution. The normal distribution analyse describes how four individual errors create an overbound of the combined error. Table 1 shows mean and one-sigma values for radial, along-track, cross-track, clock errors and URE of satellites grouped by type during 2019.

Table 1: Radial, along-track, cross-track, clock errors and URE for three types of satellites. The mean and one-sigma values are listed. All values are in centimeters.

Type	Radial		Along-track		Cross-track		Clock		URE
	μ	σ	μ	σ	μ	σ	μ	σ	σ
GEO	-20.30	1426.82	23.78	1594.59	44.03	273.21	477.12	410.67	936.45
IGSO	-55.51	960.22	-80.71	970.30	2.36	965.39	-200.92	354.69	576.76
MEO	-3.92	668.98	-57.09	683.56	0.23	680.72	-29.14	570.72	494.40

From Table 1, the distribution of these errors for different types of satellites is different. For MEO orbit errors, along-track component has the low observability in the orbit determination process and presents slightly larger error magnitude and dispersion. Compared with clock error of GEO and IGSO, biases are much smaller for MEO. The clock error distribution of GEO and IGSO has obvious bias relative to zero. For IGSO, there is a little difference existing in the orbit error dispersion and the bias of cross-track component is smaller. For GEO, radial and along-track components display almost the same error magnitude and dispersion. Comparing the σ_{URE} of GEO (9.4m), IGSO (5.8m) and MEO (4.9m), the performance of MEO is the best, followed by IGSO and GEO.

Given URE definition in equation (2), clock error component directly translates into the range error, which means range error can be greatly affected by the clock component. In order to compare nominal error performance among satellites, clock error for individual satellite should be analyzed. Table 2 provides mean and one-sigma values of orbit and clock errors for individual satellite.

Table 2: Radial, along-track, cross-track and clock errors for each satellite. The mean and one-sigma values are listed. All values are in centimeters.

Type	BeiDou Satellite ID	Radial		Along-track		Cross-track		Clock	
		μ	σ	μ	σ	μ	σ	μ	σ
GEO	C016	-43.9	1058.6	19.4	1078.3	4.2	204.1	688.0	347.6
	C018	-42.7	1262.3	-17.5	1289.6	75.2	238.7	469.1	305.2
	C006	29.2	1267.4	-7.7	1412.9	157.7	265.4	348.2	353.6
	C011	-24.0	1964.4	102.1	2323.7	-62.9	321.6	400.3	519.7
IGSO	C005	-37.4	963.1	-75.3	973.2	-5.6	954.2	-43.0	303.6
	C007	-56.4	1008.4	-93.2	1027.0	0.9	986.9	-349.7	310.0
	C008	-70.0	867.1	-98.0	885.1	0.3	938.1	-276.8	293.8
	C009	-50.3	980.3	-58.3	982.1	10.9	978.4	-309.9	324.2
	C010	-60.5	1015.4	-76.1	1017.8	1.1	976.4	-383.9	343.6
	C017	-63.6	924.7	-79.5	922.4	9.9	959.2	68.4	339.0
	C019	-49.9	953.5	-85.0	977.2	-1.2	963.7	-102.1	290.7
MEO	C012	-14.8	648.9	-60.3	644.8	-14.2	670.1	-87.3	335.6

C013	-24.8	660.1	-61.0	670.3	-20.7	695.7	-98.4	320.7
C015	-25.5	694.3	-59.6	693.6	-8.5	700.2	-168.3	322.2
C201	-2.2	642.2	-71.6	669.1	34.7	658.8	-141.3	297.8
C202	-0.9	665.1	-62.2	674.3	24.6	672.5	-559.0	426.9
C206	5.6	666.6	-58.2	664.9	24.1	670.5	-340.6	303.7
C205	-4.6	671.9	-58.5	803.8	25.0	682.3	-439.5	369.6
C209	6.9	684.9	-40.4	716.1	-19.4	720.9	-920.0	322.1
C210	11.0	676.4	-52.5	679.8	-20.6	678.5	-348.7	324.8
C212	-3.0	668.3	-57.5	668.0	-21.4	668.4	413.7	308.0
C211	1.8	682.6	-47.1	672.3	-21.5	680.7	642.0	284.3
C203	0.9	652.9	-54.2	664.1	11.9	666.1	606.0	267.4
C204	-4.1	662.1	-56.9	667.6	13.5	673.1	582.0	370.5
C207	2.3	685.5	-59.2	669.3	1.0	683.9	401.0	304.2

As shown in Table 2, distribution characteristics of error terms for single satellite are different. The clock error bias of GEO is larger than that of IGSO. Unlike the GEO and IGSO manufactured by China Aerospace Science and Technology Corporation (CASC), MEO satellites are manufactured by CASC and Shanghai Engineering Center for Microsatellites (SECM), respectively. Among fourteen MEO satellites, five satellites, i.e. C212, C211, C203, C204 and C207, are manufactured by SECM and others are manufactured by CASC. The difference between satellites made by CASC and made by SECM is onboard clock type. CASC uses Rubidium clock while SECM adopts Hydrogen clock. These five satellites have bigger clock error bias compared with remaining nine satellites, which means clock performance is not as good as that made by CASC even if SECM uses Hydrogen clock.

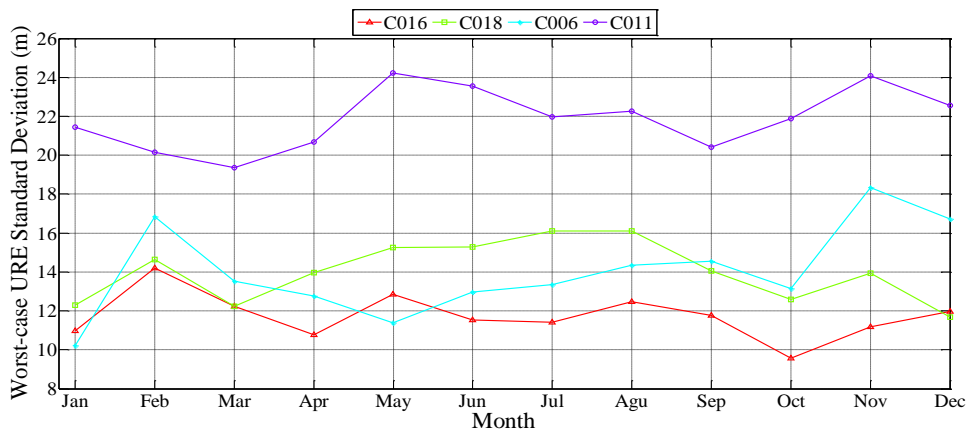


Figure 3: GEO worst-case URE monthly standard deviation

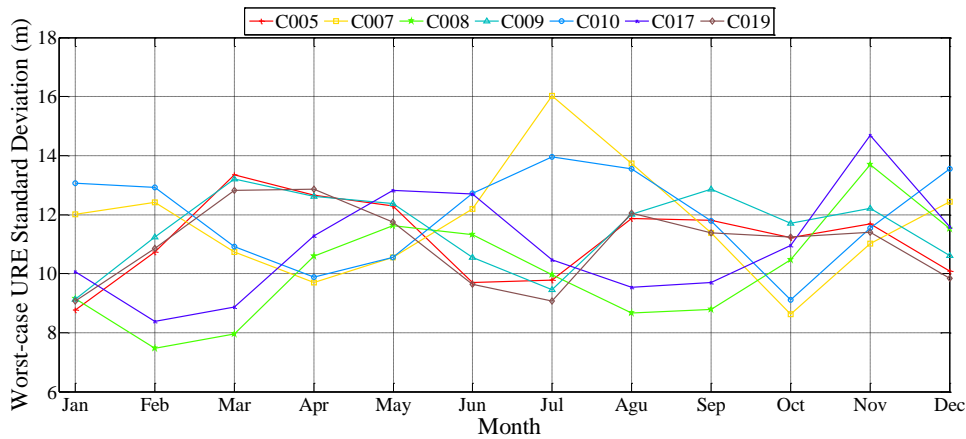


Figure 4: IGSO worst-case URE monthly standard deviation

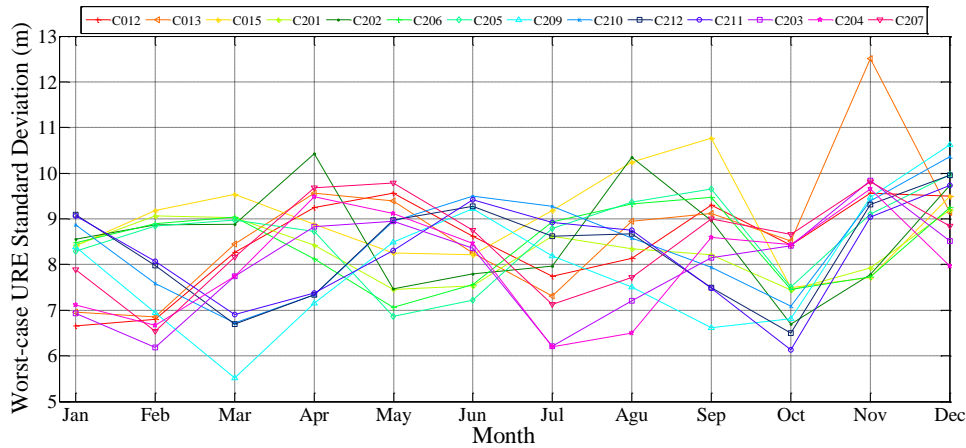


Figure 5: MEO worst-case URE monthly standard deviation

By breaking the whole year data into monthly dataset, Figures 3, 4 and 5 show corresponding values of the worst-case URE standard deviation for each individual satellite of three types. Comparing three figures, the $\sigma_{worst-case}$ of GEO is larger than IGSO and MEO especially for C011 BDS-2 satellite, which means range error fluctuates greatly and performance of GEO is not stable. For the C006 GEO satellite, the standard deviation increases more than 60% throughout the whole year and reaches highest in November 2019. The C006 was launched in November 2010 and this degradation in performance should be attributed to the proximity of satellite service life. For the C017 IGSO satellite, the standard deviation has only a small increase in the whole year but suddenly increases almost 45% in November. The same situation also happens to C007 IGSO, C008 IGSO and C013 MEO satellites whose standard deviations fluctuate by more than 30% in one month of the year. These three satellites are launched in 2010, 2011 and 2012 respectively and are at the end of service life with unstable performance. For other satellites, there is no significant change of $\sigma_{worst-case}$ during the whole year.

BDS is divided into three phases, i.e. BDS-1, BDS-2 and BDS-3. Satellites of BDS-2 and BDS-3 are still operational during 2019. Among fourteen MEO satellites, three satellites, i.e. C012, C013 and C015, belong to BDS-2. From Table 2, the bias of radial and along-track error components of BDS-2 satellites is bigger than BDS-3 while the bias of cross-track and clock error components of BDS-2 is smaller. From Figure 5, there is no significant difference of the monthly change in $\sigma_{worst-case}$ between BDS-2 and BDS-3 satellites except C013 BDS-2 satellite. For the C013 BDS-2 satellite, the standard deviation has only a small increase in the whole year but suddenly increases more than 75% in November.

Based on above analysis, the correlation of orbit and clock errors is further studied. For each type, a representative satellite is taken to generate the autocovariance plot in Figures 6-8 for C016 /GEO-6, C005 /IGSO-1 and C012 /MEO-3, respectively.

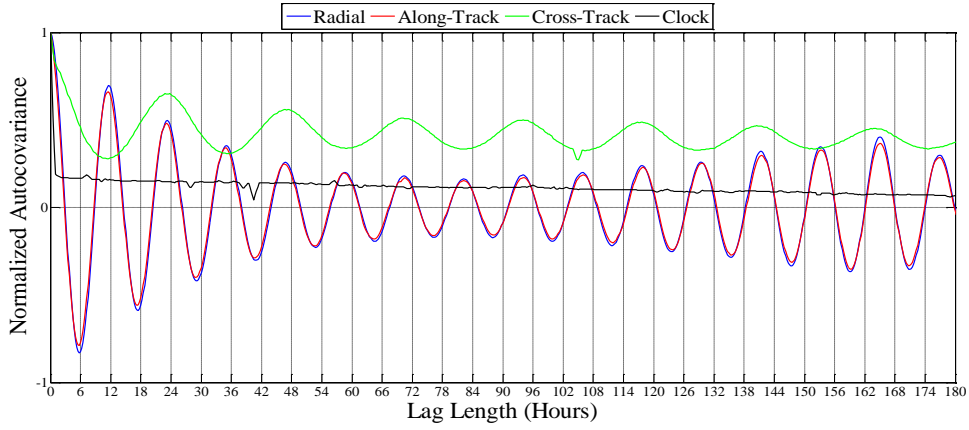


Figure 6: Sample autocovariance for C016/GEO-6 orbit and clock errors

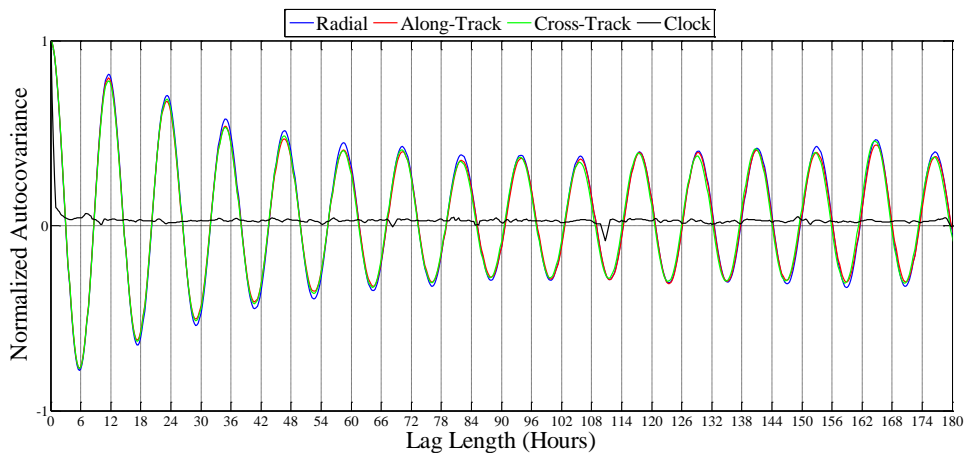


Figure 7: Sample autocovariance for C005/IGSO-1 orbit and clock errors

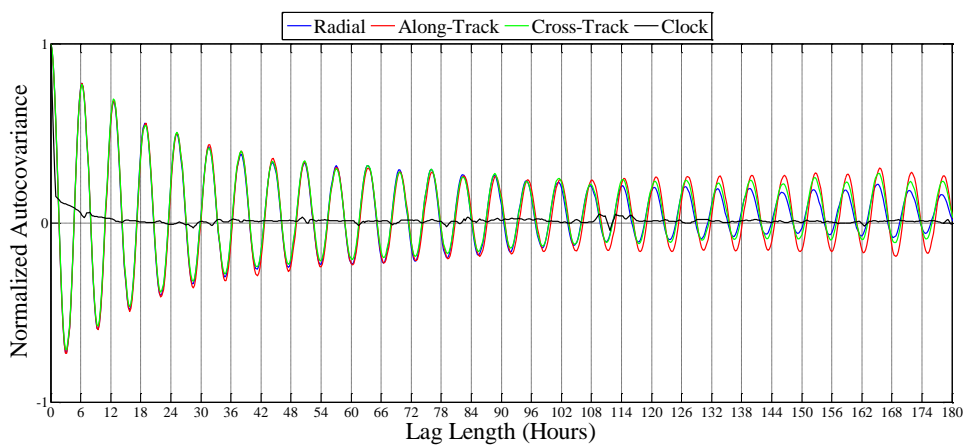


Figure 8: Sample autocovariance for C012 /MEO-3 orbit and clock errors

Orbit error, i.e., radial, along-track and cross-track errors, shows significant disparity about periodicity between satellite types. A 12-h harmonic component is observed for both IGSO and GEO orbit errors, while the harmonic component in MEO orbit error corresponds to the 6-h frequency. The cross-track error shows a 24-h sinusoidal behavior for GEO. Like orbit components, the clock autocovariance between satellite types also exists large difference on the convergence time. The sinusoidal components of MEO and IGSO clock error decay faster than GEO.

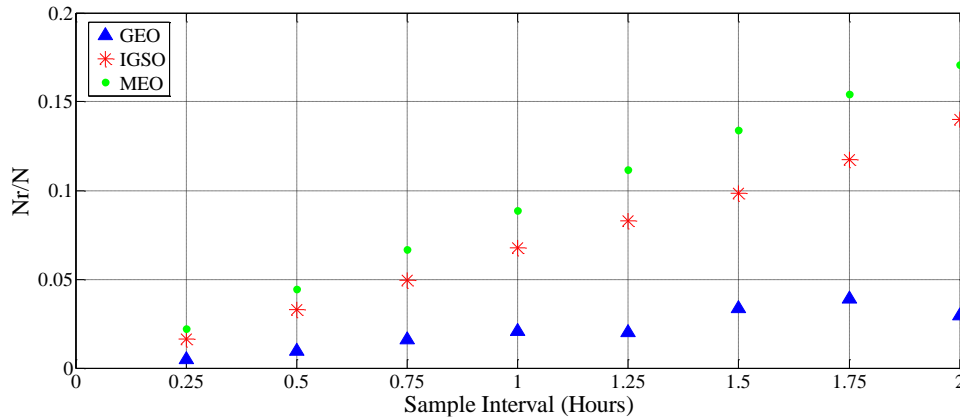


Figure 9: Ratio of Independent samples for BDS (GEO, IGSO and MEO)

Figure 9 presents the values of N_r/N for GEO, IGSO and MEO. N_r/N is monotonous function of the sampling interval and different sampling interval can only affect the number of selected samples but not the number of effectively independent samples in the analysis period. According to equation (7), the time between independent samples for GEO ranges from 44 to 67 hours. The time interval for IGSO is from 14 to 15 hours and for MEO is from 11 to 12 hours. From the result, the independent sample interval is highly dependent on satellite type.

CONCLUSIONS

The nominal performance of BDS is firstly evaluated by comparing the broadcast and precise ephemerides for one year to calculate URE. The nominal range error of 14 BDS-2 and 11 BDS-3 satellites is analyzed. Then performance of different types of satellites is analyzed to determine the statistical parameters of orbit and clock errors. These errors vary with satellite type and by individual satellite. Since MEO satellites are produced by two manufacturers respectively carrying either rubidium or hydrogen clocks, satellites made by SECM have larger clock error bias compared with satellites made by CASC. Comparing the σ_{URE} of GEO (9.4m), IGSO (5.8m) and MEO (4.9m), the performance of MEO is the best, followed by IGSO and GEO.

The BeiDou service history is broken down into monthly dataset to analyze the variation of single satellite performance during the whole year. One of the GEO satellites degrades more than 60% due to the proximity of satellite service life. For C017, C007, C008 and C013 satellites, the standard deviation has only a small increase in the whole year but fluctuates by more than 30% in one month of the year. No significant difference is identified for other satellites after one year. Because the worst-case URE standard deviation of satellite at the end of life shows a strong time variation, the setting of update time for ISM parameters should be based on the most unstable satellite. Compared with BDS-3 satellites, the bias of radial and along-track error components is bigger for BDS-2 satellites while the bias of cross-track and clock error components is smaller.

Based on the analysis, the correlation of orbit and clock errors for BeiDou satellites is further studied. A 12-h harmonic component is observed for both IGSO and GEO orbit errors, while the harmonic component in MEO orbit error corresponds to

the 6-h frequency. The cross-track error of GEO shows a 24-h sinusoidal behavior. Meanwhile, the MEO and IGSO clock error sinusoidal components decay faster than GEO. The independent sample interval is estimated and the time between independent samples for GEO, IGSO and MEO ranges from 44 to 67, 14 to 15 and 11 to 12 hours, respectively. The result shows independent sample interval is highly dependent on satellite type.

ACKNOWLEDGMENT

The work in this paper is funded by NSFC (Grant no. 42004029). The support is gratefully acknowledged.

REFERENCES

1. Working Group C, ARAIM Technical Subgroup, EU-US Cooperation in Satellite Navigation, "Milestone 3 report," Tech. Rep., March 2016.
2. Blanch, J., Walter, T., Enge, P., Lee, Y., Pervan, B., Rippl, M., and Spletter, A., "Advanced RAIM User Algorithm Description: Integrity Support Message Processing, Fault Detection, Exclusion, and Protection Level Calculation," *Proceedings of 25th International Technical Meeting of the Satellite Division of The Institute of Navigation (ION GNSS+ 2012)*, Nashville, TN, September 2012, pp. 2828-2849.
3. Walter, T. and Blanch, J., "Characterization of GPS Clock and Ephemeris Errors to support ARAIM," *Proceedings of the ION 2015 Pacific PNT Meeting, Honolulu, HI, April 2015*, pp. 920-931.
4. Walter, T., Gunning, K., Phelts, R., and Blanch, J., "Validation of the Unfaulted Error Bounds for ARAIM," *NAVIGATION*, Vol. 65, 2018, pp. 117-133.
5. Perea, S., Meurer, M., Martini, I., Rippl, M., Joerger, M., and Pervan, B., "Nominal Range Error Analysis to support ARAIM," *Proceedings of 29th International Technical Meeting of the Satellite Division of The Institute of Navigation (ION GNSS+ 2016)*, Portland, OR, September 2016, pp. 1726-1735.
6. Perea, S., Meurer, M., Rippl, M., Belabbas, B., Joerger, M., and Pervan, B., "URA/SISA Analysis for GPS-Galileo ARAIM Integrity Support Message," *Proceedings of 28th International Technical Meeting of the Satellite Division of The Institute of Navigation (ION GNSS+ 2015)*, Tampa, FL, September 2015, pp. 735-745.
7. Perea, S., Meurer, M., and Pervan, B., "Impact of sample correlation on SISRE overbound for ARAIM," *NAVIGATION*, Vol. 67, 2020, pp. 197-212.
8. Zhang, Q., Sui, L., Jia, X., and Zhu, Y., "SIS Error Statistical Analysis of Beidou Satellite Navigation System," *Geomatics & Information Science of Wuhan University*, Vol. 423, 2014, pp. 175-188.
9. Mistrapau, F., Bija, B., Cueto-Felgueroso, G., Odriozola, M., Azaola, M., Cezón, A., and Amarillo-Fernández, F., "GPS SISRE/URA Integrity Analysis for ARAIM," *Proceedings of 29th International Technical Meeting of the Satellite Division of The Institute of Navigation (ION GNSS+ 2016)*, Portland, OR, September 2016, pp. 1793-1803.
10. Montenbruck, O., Steigenberger, P., and Hauschild, A., "Broadcast versus precise ephemerides: a multi-GNSS perspective," *GPS Solutions*, Vol. 19, 2015, pp. 321-333.
11. Heng, L., Gao, G. X., Walter, T., and Enge, P., "GPS Signal-in-Space Anomalies in the Last Decade: Data Mining of 400,000,000 GPS Navigation Messages," *Proceedings of 23th International Technical Meeting of the Satellite Division of The Institute of Navigation (ION GNSS+ 2010)*, Portland, OR, September 2010, pp. 3115-3122.
12. *BeiDou Navigation Satellite System Signal In Space Interface Control Document Open Service Signal (Version 2.1)*, China Satellite Navigation Office, November 2016.
13. *BeiDou Navigation Satellite System Signal In Space Interface Control Document Open Service Signals B1C and B2a (Test Version)*, China Satellite Navigation Office, August 2017.

14. Wu, Y., Liu, X., Liu, W., Ren, J., Lou, Y., Dai, X., and Fang, X., "Long-term behavior and statistical characterization of BeiDou signal-in-space errors," *GPS Solutions*, Vol. 21, 2017, pp. 1907-1922.
15. Wang, Z., Shao, W., Wang, S., and Zheng, L., "Statistical Analysis of User Range Errors on BDS for ARAIM," *Proceedings of 31th International Technical Meeting of the Satellite Division of The Institute of Navigation (ION GNSS+ 2018)*, Reston, VA, January 2018, pp. 72-87.
16. *Global Positioning System Standard Position Service Performance Standard*, U.S. Department of Defense, 4th Edition, September 2008.
17. Chen, L., Jiao, W., Huang, X., Geng, C., Ai, L., Lu, L., and Hu, Z., "Study on Signal-In-Space Errors Calculation Method and Statistical Characterization of BeiDou Navigation Satellite System," *Proceedings of 4th China Satellite Navigation Conference (CSNC 2013)*, Wuhan, HB, May 2013, pp. 423-434.
18. Test and Assessment Research Center of China Satellite Navigation Office,
"http://www.csno-tarc.cn/system/constellation."